frontiers | Frontiers in Earth Science

TYPE Original Research
PUBLISHED 13 January 2023
DOI 10.3389/feart.2022.1003818

OPEN ACCESS

EDITED BY
Lawrence H. Tanner,
Le Moyne College, United States

REVIEWED BY
Wan Hanna Melini Wan Mohtar,
Universiti Kebangsaan Malaysia, Malaysia
J. Richard Bowersox,
University of Kentucky, United States

*CORRESPONDENCE
Zhen Yang,
yangzhen@stumail.nwu.edu.cn

SPECIALTY SECTION
This article was submitted to Sedimentology, Stratigraphy and Diagenesis, a section of the journal Frontiers in Earth Science

RECEIVED 26 July 2022
ACCEPTED 01 November 2022
PUBLISHED 13 January 2023

CITATION
Yang Z, Wang S, Chen J and Jing S (2023), Architecture, genesis, and the sedimentary evolution model of a single sand body in tight sandstone reservoirs: A case from the Permian Shan-1–He 8 members in the northwest Ordos Basin, China.
Front. Earth Sci. 10:1003818.
doi: 10.3389/feart.2022.1003818

Architecture, genesis, and the sedimentary evolution model of a single sand body in tight sandstone reservoirs: A case from the Permian Shan-1–He 8 members in the northwest Ordos Basin, China

Zhen Yang[1]*, Shumin Wang[2], Jiahao Chen[3,4] and Shuai Jing[5]

[1]Department of Geology, Northwest University, Xi'an, China, [2]Exploration and Development Research Institute, PetroChina Changqing Oilfield Company, Xi'an, China, [3]Faculty of Earth Resources, China University of Geosciences, Wuhan, China, [4]College of Geosciences, China University of Petroleum, Beijing, China, [5]The Second Natural Gas Plant, Shaanxi Yanchang Oil and Gas Exploration Company, Yulin, China

A single sand body is defined as a geological unit that is continuous vertically and horizontally but separated from the upper and lower sand bodies by mudstone or impermeable intercalation. The architecture of a single sand body is significant in the determination of hydrocarbon accumulation mechanisms in gas reservoirs, especially for exploitation of multiple tight sandstone gas (TSG) reservoirs. One such example is the gas reservoirs in the Tianhuan Depression, China, where the architecture and genesis of sand bodies are poorly understood. Based on the geologic background and sedimentary characteristics, the evolution of the distributary channel in the Tianhuan Depression has been examined using data from geological outcrops, cores, and well logs. The results showed that sand body architecture depends on the evolution of channel systems, and the scale and size of the channel are controlled by the sedimentary environment. Three kinds of sedimentary microfacies (distributary channel, channel mouth bar, and interdistributary bay) are mainly developed in the study area, and four types of single sand body stacking patterns (isolated, vertically superimposed, laterally tangentially superimposed, and horizontally bridged sand bodies) have formed in such a depositional environment. The target strata (Shan-1 and He-8 members) provide an ideal object for studying the evolution of the river and the architecture of the sand bodies. During the early stage of deposition, the sediment supply was insufficient, with restricted meandering river deltas dominating and sand bodies mostly existing as isolated types. Until the middle period of deposition, the sediment supply suddenly increased, the sedimentation rate accelerated with the decrease in the lake water base level, and the channel evolved into a large-scale braided river delta, generally forming superimposed sand bodies. By the late period of deposition, the provenance supply was reduced again; although braided

river delta deposits were still dominant, the channel scale was restricted, and the sand bodies were predominantly isolated and horizontally bridged types. This work establishes a sedimentary evolution model for tight sandstone gas reservoirs, that is, a complete cycle of river evolution from small scale to large scale to terminal weakening, and discusses the genetic mechanism of single sand body architecture in such a depositional model.

KEYWORDS

single sand body, tight sandstone gas reservoirs, sand body architecture, distributary channel, sedimentary evolution, Ordos Basin

1 Introduction

A single sand body is defined as a geological unit that is continuous vertically and horizontally but separated from the upper and lower sand bodies by mudstone or impermeable intercalation (Colombera and Mountney, 2021). An understanding of the single sand body architecture underpins the successful exploitation of many hydrocarbon resources (Allen, 1978), particularly when secondary or tertiary recovery is contemplated. Different sand bodies vary considerably in grain size, sorting, and impurity content, which lead to great differences in the reservoir's physical properties (Pranter and Sommer, 2011). In addition, sand bodies are often separated by thin mudstones, argillaceous siltstones, or argillaceous fine sandstones, resulting in disconnection between sand bodies and strengthening reservoir heterogeneity (Hovadik and Larue, 2007; Heidsiek et al., 2020). The distribution characteristics of sand bodies are entirely determined by paleochannel evolution, with channel swings and breaches being basic characteristics of sedimentary basin filling (Jerolmack and Mohrig, 2007; Hajek and Edmonds, 2014). Quantitatively characterizing the evolutionary stages of rivers and the superposition relationships of channels is an important means to understand the fluid migration pathways in sand bodies (Toorenenburg et al., 2016; Pisel et al., 2018). More importantly, sand body architecture affects the connectivity of subsurface reservoirs. It has profound implications for strategic schemes such as CO_2 sequestration, hydrocarbon extraction, and hydrothermal heating (Syvitski et al., 2012; Sahoo et al., 2020).

The river systems are built over longer periods owing to repeated migration and rerouting, and subsequent new channels are developed on the original abandoned channels (Aslan et al., 2005; Coronel et al., 2020). Previous studies have shown that the style and distribution of channelized sand bodies are controlled by heterologous (external) factors such as tectonic subsidence, relative sea level, basin subsidence, climate and hinterland tectonism (Aalto et al., 2003; Flood and Hampson, 2017), and autogenic behaviors, such as avulsion (Galina and Norman, 2000; Hajek and Wolinsky, 2012). Numerical models investigating the origin of channelized sand bodies show that provenance supply, erosion frequency, and accumulation rate jointly control the spatial distribution of underwater sand bodies in delta plain strata (Blum et al., 2013; Tye, 2013). Predictive sand body architecture focuses on emphasizing that their stratigraphic framework is primarily driven by cyclical changes in relative sea level (Fernandes et al., 2016). In addition, the sand body architecture downstream of the river is more susceptible to slope and topography, while upstream is more affected by heterologous climatic and tectonic controls (Hajek and Wolinsky, 2012; Shen et al., 2015; Widera, 2016). The thickness of the channel's lateral thin sand is equivalent to the weaker multi-layer sand accumulation. Its thickness is proportional to the channel depth (Pranter et al., 2009; Flood and Hampson, 2015), and the width of sand bodies is determined by the river scale and alluvial stage (Gibling, 2006). In addition, compensational stacking of sand bodies is preferentially carried out at lower topographical locations due to differential deposition rates, which are dependent on the original sedimentary environment and provenance conditions (Miall, 1977; Slingerland and Smith, 1998; Roberts, 2007). However, current interpretations about the architecture and genesis of single sand bodies emphasize the various allogenic controls (Hampson et al., 2012), while authigenic determinants such as the original depositional environment have been neglected, especially the process and mechanism of channel evolution, which remain unclear.

The northern Tianhuan (NT) Depression is a super-large gas field in the Ordos Basin, Central China (Yang et al., 2012), whereas the accuracy criteria based on single-layer scale can no longer meet the demands of reservoir exploration, especially in the development of tight sandstone gas reservoirs, where the basic geological unit has shifted from single-layer to single sand body within compound channels (Dai et al., 2012; Meng et al., 2016; Zhu et al., 2020). Although many studies have documented characteristics regarding the scale and type of sand bodies and paleochannels (Zhang et al., 2018; Zhu et al., 2020), the key determinants of sand body architecture (processes and mechanisms of channel evolution) remain unclear. Hence, we investigated the following: 1) the sand body architecture, namely, the sand body stacking styles, and the systematic classification of sedimentary microfacies in the study area. 2) The processes and models of sedimentary evolution. 3) The genesis of the single sand body and the channel evolution mechanism through the analysis of comprehensive geological factors such as outcrops, cores, and well logging data, concerning the geological evolution background.

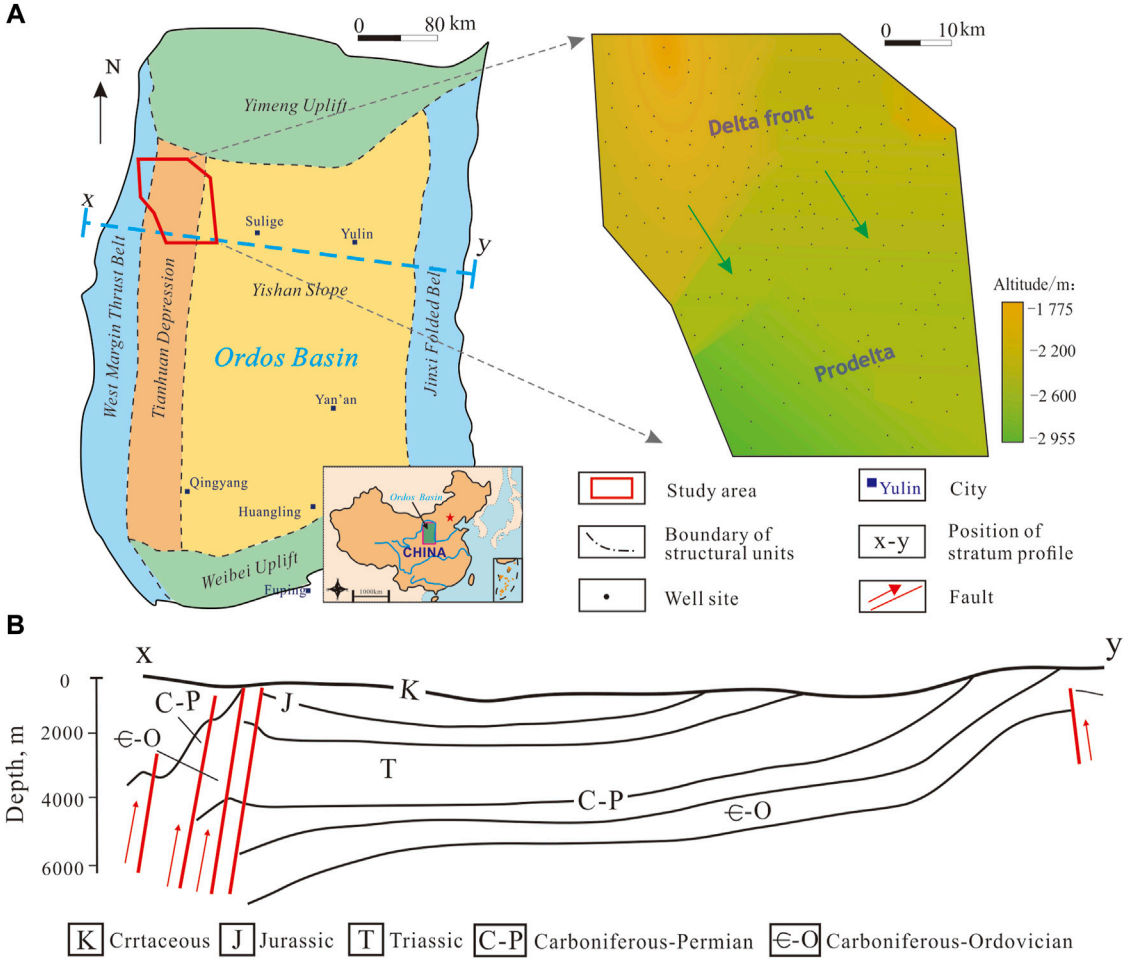

FIGURE 1
Geographical location of the study area and structural units of the Ordos Basin. **(A)** Location of the study area. The study area is an irregular polygon due to the topography limitations of the Western Margin Thrust Belt and the distribution of exploration wells. **(B)** Distribution of strata and faults through the line x-y.

2 Geological setting

The Ordos Basin is located in Central China (Figure 1) to the west of the Lvliang Mountains and east of the Helan Mountains (Zhu et al., 2013; Zhou et al., 2016). The Ordos Basin can be divided into six different tectonic settings, namely, the Yimeng Uplift, the Western Margin Thrust Belt, the Tianhuan Depression, the Weibei Uplift, the Jinxi Folded Belt, and the Yishan Slope, of which the Yishan Slope has relatively stable tectonic subsidence (Yang et al., 2008). The slope and adjacent Tianhuan Depression areas are considered the primary tight gas reservoirs for the next 30 years (Guo et al., 2016).

The study area, the NT Depression, is in the northwestern Ordos Basin, covering approximately 11,000 km^2. The study area is adjacent to the Sulige gas field in the east and connected to the Western Margin Thrust Belt in the west. The upper Paleozoic strata are a set of clastic rock sedimentary systems with marine and continental transition facies (Gao et al., 2019). The Permian strata are successively developed into the Taiyuan Formation (P_1t), the Shanxi Formation (P_2s), the Lower Shihezi Formation, and the Upper Shihezi Formation (P_2h), with a total sedimentary thickness of approximately 500 m (Figure 2). The source rocks are mainly coal seams and dark mudstone of the Taiyuan–Shanxi formations, which have the characteristics of extensive hydrocarbon generation (Xiao et al., 2005). The high-yield gas reservoirs are mainly produced from the Shanxi and Lower Shihezi formations (Yang et al., 2008). The 1st to 7th members (He 1 to He 7) of the P_2h are the regional cap rocks. The main gas-producing strata are the 1st member of the Shanxi Formation (Shan 1, the following are denoted by "Sh-1") and the 8th member of the Xiashihezi Formation (He 8), among which He 8 can be further subdivided into the upper and

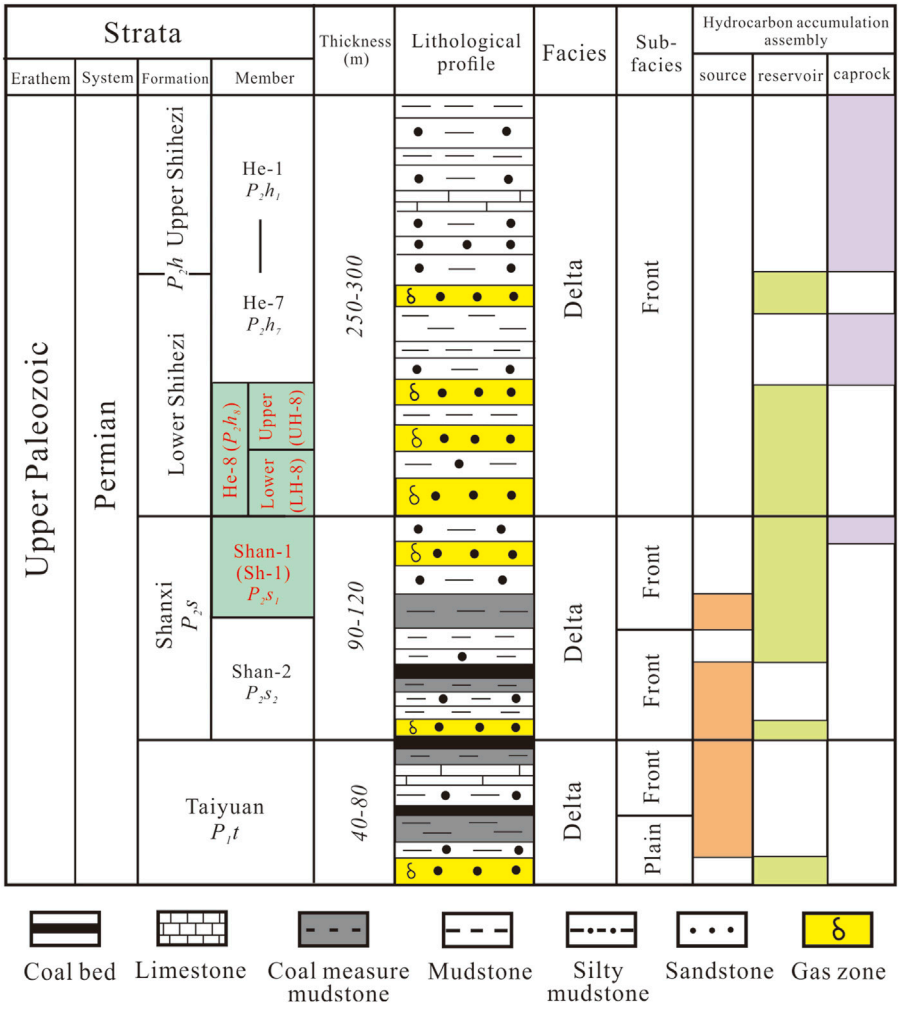

FIGURE 2
Comprehensive stratigraphic column of the study area. The Lower Shihezi Formation's 8th member (He-8, subdivided into "UH-8" and "LH-8") and the Shanxi Formation's 1st member (Shan-1, referred to as "Sh-1") are highlighted in red.

lower He 8 (the following are denoted by "UH-8" and "LH-8"). The Sh-1 formation developed as shallow meandering river delta deposits, while the He-8 formation developed as shallow braided river delta deposits (Tian et al., 2011), both of which are regionally superimposed contacts.

3 Materials and methods

3.1 Outcrop measurement

The advantages of field outcrop research, such as visualization, large-scale, and high precision, are unmatched by other reservoir configuration research methods. To obtain channel scale data and sand bodies' distribution patterns, we selected two outcrop sites with complete Sh-1 and He-8 members and rich geological phenomena on the section and selected 14 observation points for mapping, recording, and systematic photographing. The GTA 1800R Electronic Total Station was used to measure the thickness and width of distributary channel sand bodies exposed in the outcrop section, and formation azimuth and dip angle were measured using an HG31 Compass to correct the distributary channel width to obtain the true and accurate parameters of the distributary channel.

3.2. Width-to-thickness ratio

Hydrodynamic conditions control the depth and width of the channel, which in turn affect the thickness of the single sand body and the width of the channel zone (Gibling, 2006). The study of

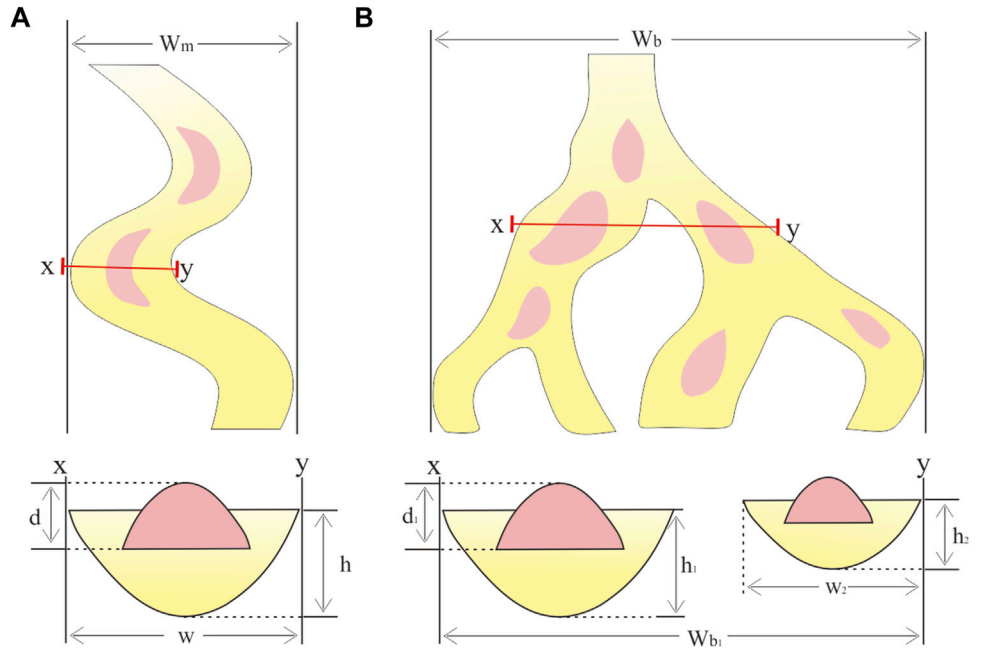

FIGURE 3
Schematic diagram of the delta channel width calculation process. **(A)** shows a single meandering river model, which is used to calculate the channel width of the Sh-1 member. **(B)** shows a multi-channel braided river model, which is used to calculate the channel width of the He-8 member.

river geology and geomorphology shows that the height of the channel mouth bar is controlled by the flow depth when the river is at its full bank (Weerts and Bierkens, 1993; Turner and Tester, 2006), and the channel width is positively correlated with the water depth (Figure 3).

In this study, based on outcrops, cores, and logging methods, we identified and counted the scale of channel mouth bars and sand bodies and successfully predicted the channel width and sand body connectivity by using the established width–thickness ratio range in the study area (Tian et al., 2013). It is calculated using Eqs 1 and 2 for the single river and Eqs 3–5 for the multi-phase channel belt. The calculation process is as follows:

$$h = 1.5 \times d, \tag{1}$$

$$w = 6.75 \times h^{1.54}, \tag{2}$$

where h is the depth of the river, d is the thickness of the channel mouth bar, and w is the width of the river.

$$W_m = 65.5 \times D^{1.54}, \tag{3}$$

$$W_b = 59.9 \times D^{1.8}, \tag{4}$$

$$D = 1/n \times (h_1 + h_2 + h_2 + \ldots\ldots + h_n), \tag{5}$$

where W_m is the channel-belt width of a meandering river, W_b is the channel-belt width of a braided river, and D is the average depth of the channel.

4 Results

4.1 Sedimentary microfacies

Delta plain and front sub-facies are mainly deposited in the Tianhuan Depression. According to the comprehensive comparison of field outcrops, cores, and logging data and referring to the identification principles of typical sedimentary environment, the classification standards for sedimentary microfacies in the study area were established (Table 1). Three kinds of sedimentary microfacies are mainly developed: the distributary channel, the channel mouth bar, and the interdistributary bay.

4.1.1 Distributary channel

The lithology of the distributary channel is dominated by medium sandstone and fine sandstone, and the stranded coarse sandstone is deposited at the bottom of the single sand body (Figure 4). The sedimentary structures include parallel bedding, small tabular cross-bedding, and wedge cross-bedding. Scour surfaces or mud gravel deposits can also be seen on outcrops and cores. The vertical direction is mainly positive rhythm, that is, the sandstone grain size tapers upward. Corresponding to the logging response, the resistivity (RT) curve exhibits a box shape of medium-to-high amplitude (Figure 4).

TABLE 1 Classification standard of delta sedimentary microfacies in the Sh-1 to He-8 members, the Tianhuan Depression.

Sub-facies	Sedimentary microfacies	Lithology	Sedimentary structure	Vertical rhythm	Logging response
Delta plain and delta	Distributary channel	Med-sandstone Fine sandstone	Parallel bedding, cross-bedding, scour surface, and mud gravel	Positive	Low SP and high RT
	Channel mouth bar	Med-sandstone Fine sandstone	Cross-bedding Mud gravel	Reverse	Low-mid SP and mid-high RT
	Interdistributary bay	Argillaceous siltstone and mudstone	Horizontal bedding	Compound	High SP and low RT

4.1.2 Channel mouth bar

The channel mouth bar is developed at the front end of underwater distributary channel, and it is formed by the rapid accumulation of sediments in the estuary due to the sudden increase of accommodating space and the decrease of flow velocity (Tian et al., 2013; Trendell et al., 2013), where the hydrodynamic force is the strongest. The lithology is basically medium-fine sandstone. The grain size is fine at the bottom and coarse at the top (reverse rhythm), and the channel mouth bar is crescent-shaped in the plane and lens-shaped in the section. Small wedge cross-bedding, tabular cross-bedding, and mud gravel structures are developed. Corresponding to the logging response, the spontaneous potential (SP) curve exhibits a low-to-medium amplitude funnel shape, while the RT curve exhibits a medium-to-high amplitude funnel shape (Figure 4).

4.1.3 Interdistributary bay

The interdistributary bay is a relatively low-lying area between distributary channels or mouth bars, which is poorly connected with the external water and is generally shallow. It is the main barrier and interlayer in the delta plain. The lithology is dominated by argillaceous siltstone and mudstone, and horizontal bedding is common. Corresponding to the logging response, the SP curve behaves more closely to the mudstone baseline (MB) (Figure 4).

4.2 Stacking pattern of a single sand body

The stacking relationship of sand bodies from Sh-1 to He-8 in the NT is divided into four main types: isolated, vertically superimposed, laterally tangentially superimposed, and horizontally bridged sand bodies (Figure 5).

The isolated sand body generally represented a single channel that experienced rapid deposition (Figure 5A) (Khalifa and Mills, 2020; Abdel, 2021), and 44% of the sand bodies in the Sh-1 member are of this type (Figure 6), typically deposited in interdistributary bays and small distributary channel environments. The vertically superimposed sand bodies showed a weak swing in the amplitude of a single channel where sediment supply is sufficient and stable (Figure 5B), while a strong oscillation will evolve into laterally tangentially superimposed sand bodies (Figure 5C) (El-Ghali et al., 2009; Snedden, 2013). The vertically superimposed and laterally tangentially superimposed sand bodies account for 38% and 37% of the LH-8 member, respectively, and are usually deposited in distributary channels and channel mouth bar settings. The horizontally bridged sand bodies represent a distributary channel with changing flow direction in multiple periods, but the duration of the single-stage channel and sediment deposition time is relatively long (Figure 5D) (Dalrymple and Choi, 2007; Marion et al., 2020); 37% of the sand bodies in the UH-8 member are of this type (Figure 6), which are mostly found in two-phase distributary channel microfacies with little tectonic elevation difference.

4.3 Distribution of sand bodies

Four to five main channels were developed in the Sh-1 member, with a width of about 1,000 m. As the channel advanced toward the lake basin, the main distributary channel further bifurcated and the number of distributary channels increased, while the size of the channel gradually decreased. The sand bodies were predominantly isolated vertically. The width of the sub-channels was approximately 200 m, and then they entered the pre-delta environment in the southeast direction (Figure 7A).

The LH-8 member was a braided river delta deposit with sufficient provenance and wide channel distribution; the whole area was covered in delta front deposition (Figure 7B). Due to the continuous migration, avulsion, and relocation of braided rivers, channel sand bodies were superimposed vertically and intertwined horizontally (Figure 7D). The scale of distributary channels gradually decreased toward the lake basin, with a reduction in the extent of lateral connectivity of the channels, and gradually evolved into multiple single channels.

During the deposition stage of the UH-8 member, the channel scale of the braided river decreased, and the size of the sand bodies was limited. The braided river was cross-divided horizontally and dominated by horizontal bridged sand bodies vertically, bridged types, and entered the pre-delta in the southeast direction (Figures 7C, D).

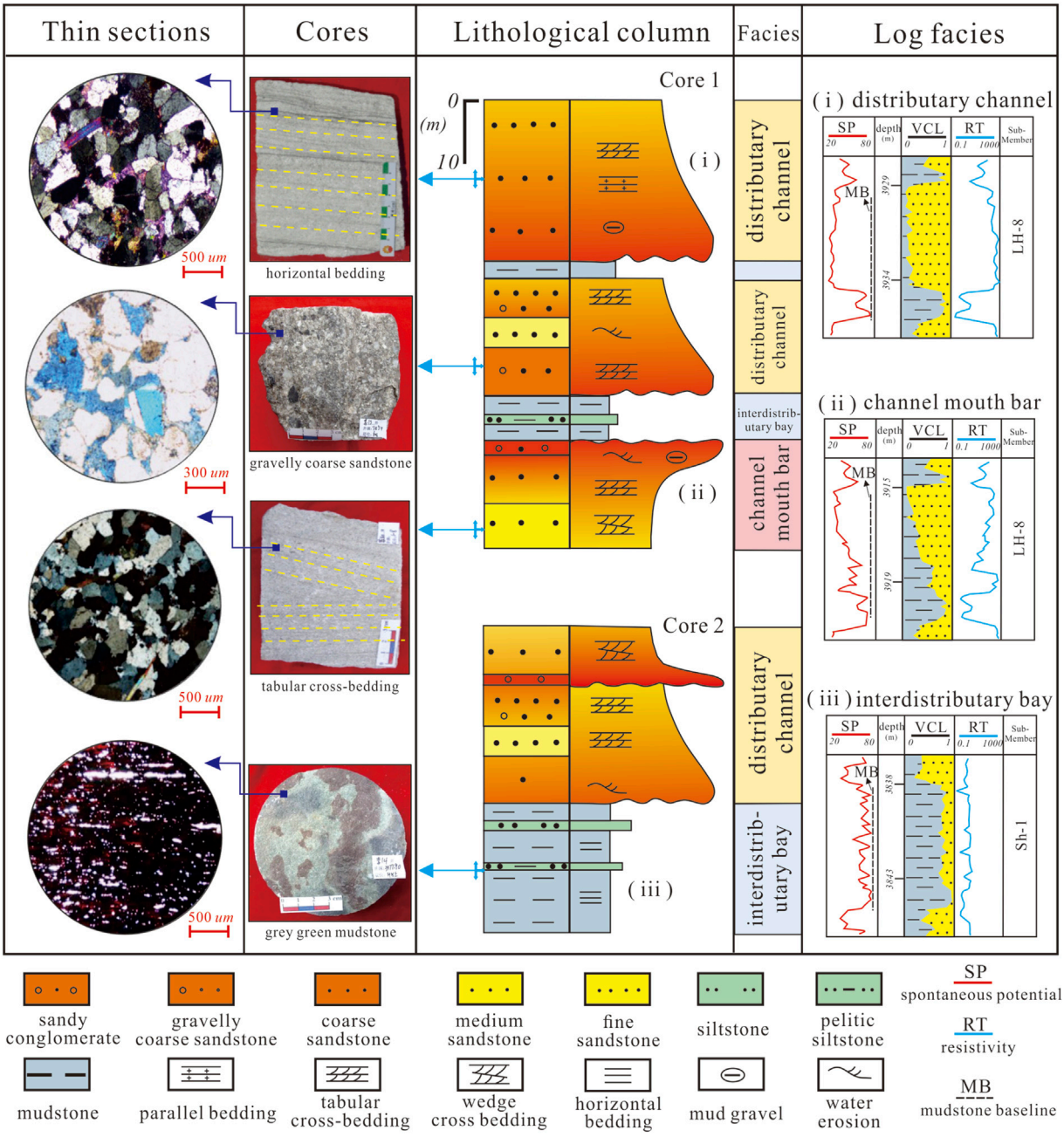

FIGURE 4
Delta plain and delta front sub-facies markers in the Sh-1 to He-8 members.

The results of quantitative calculations show that the single sand body scale (thickness and width) of the Sh-1 member was smaller than that of the He-8 member, especially the channel size of the LH-8 member, which was the largest (Table 2), indicating that the LH-8 was stronger than the UH-8 in terms of hydrodynamics. The channel scale and hydrodynamic conditions of the Sh-1 member were the weakest.

5 Discussion

5.1 Sedimentary evolution model

According to the sedimentary environments and channel variations, the provenance supply of the study area primarily came from the north and west. In the north, the terrain was gentle, and several underwater distributary channels advanced

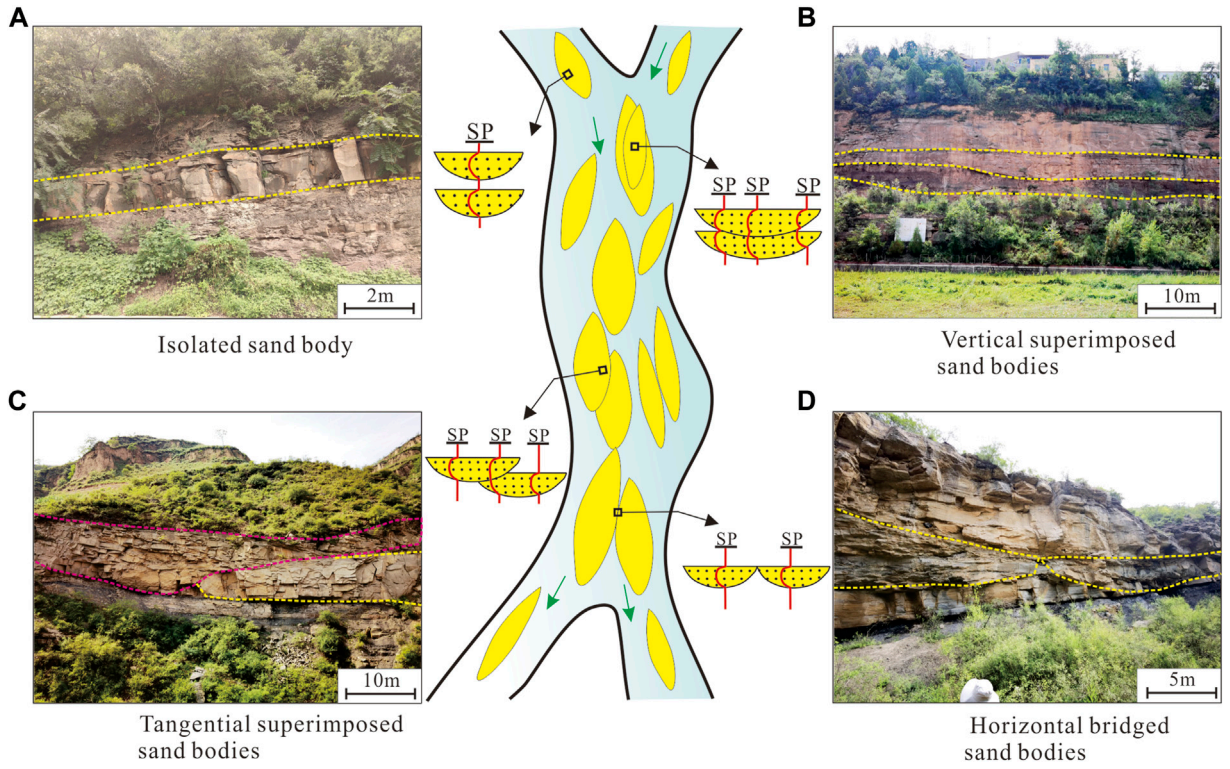

FIGURE 5
Main stacking types and outcrop characteristics of a single sand body in the study area. **(A)** Isolated sand body, **(B)** vertically superimposed sand bodies, **(C)** tangentially superimposed sand bodies, and **(D)** horizontally bridged sand bodies.

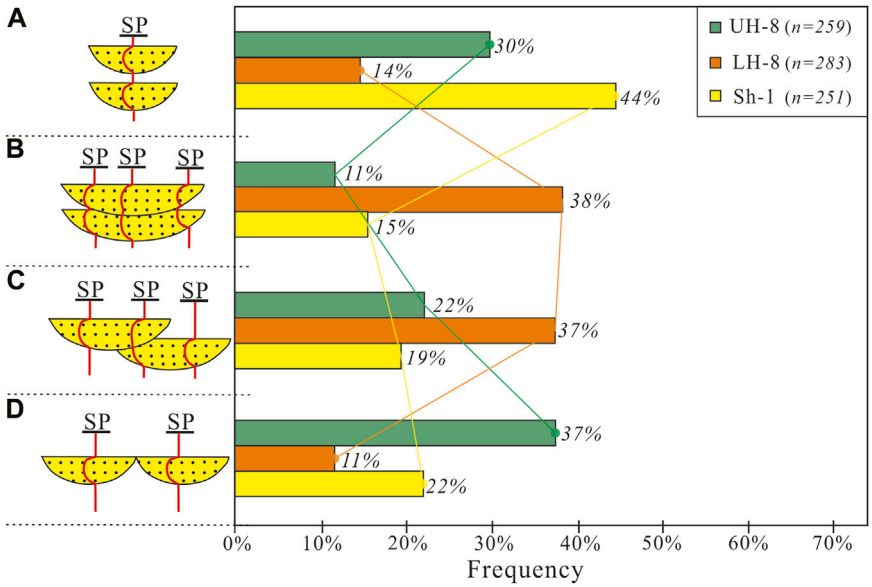

FIGURE 6
Frequency distribution of sand body stacking styles in the Sh-1 and He-8 members. **(A)** Isolated sand body, **(B)** vertically superimposed sand bodies, **(C)** tangentially superimposed sand bodies, and **(D)** horizontally bridged sand bodies. The data were obtained from logging data analysis of 88 exploration wells, including 259 complete sand bodies in the UH-8 member, 283 in the LH-8 member, and 251 in the Sh-1 member.

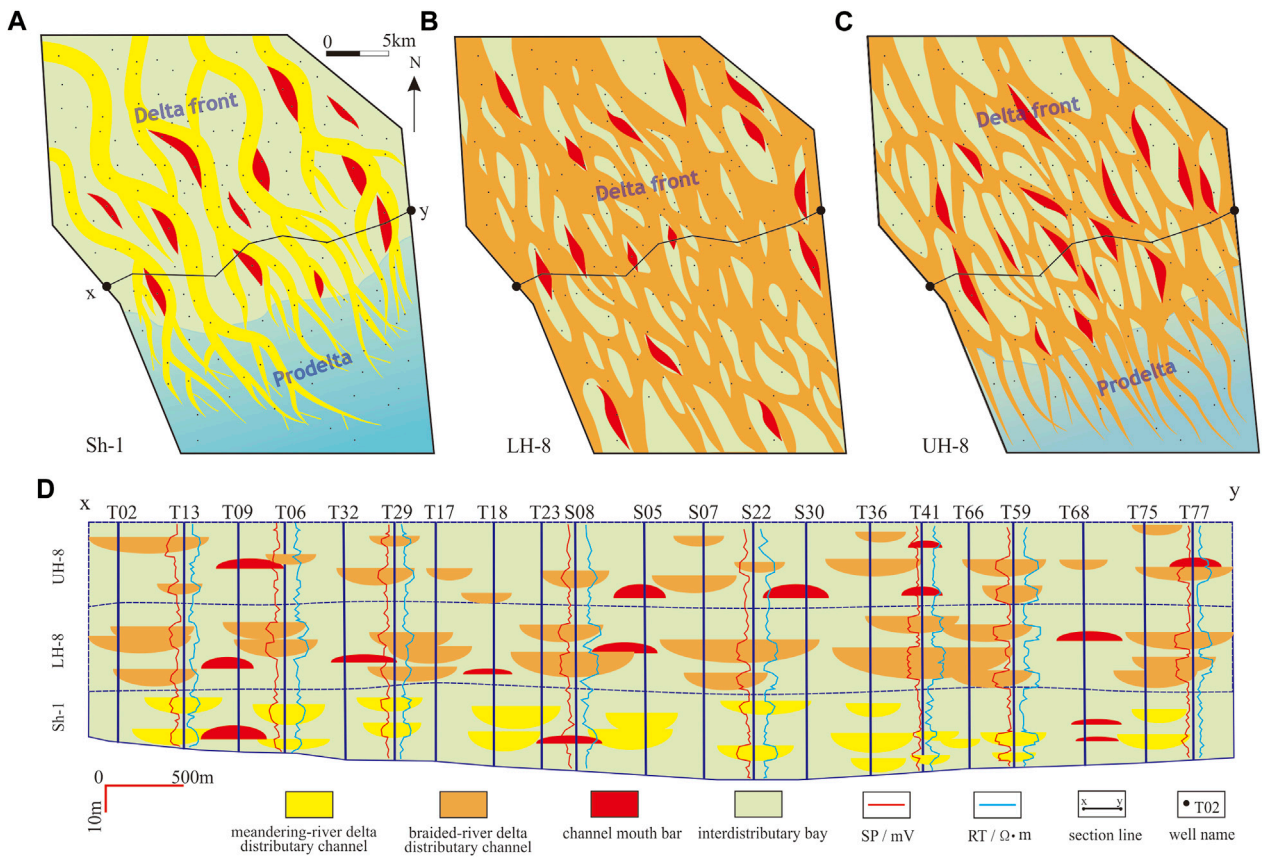

FIGURE 7
2D and vertical distribution characteristics of the delta in the Sh-1 to He-8 members. **(A–C)** represent the 2D distribution of sand bodies in the Sh-1 member, LH-8 member, and UH-8 member, respectively. **(D)** The profile of sedimentary microfacies passing through the line x-y.

TABLE 2 Quantitative calculation results of distributary channel width in the study area.

Member	Sand body thickness (m)			Channel width (m)			Channel zone width (m)		
	Min	Max	Avg int	Min	Max	Avg int	Min	Max	Avg int
UH-8	0.8	9.8	4.1~6.2	9.3	480.5	90~205	46.5	3659.7	890~2400
LH-8	1.3	11.7	5.3~7.4	14.9	625.7	190~310	75.9	6358.2	1760~2920
Sh-1	0.7	8.4	3.9~6.1	8.6	437.6	95~180	43.2	3025.8	720~1800

Min, minimum; Max, maximum; and Avg int, average interval.

toward the center of the lake basin, forming many strip-shaped and sheet-shaped sand bodies, which were typical shallow-water delta deposits. Based on the abovementioned analysis and previous understanding of the paleoclimate and paleogeography of the Ordos Basin (Dai et al., 2012; Meng et al., 2016), a sedimentary evolution model of Sh-1 and He-8 members in the Tianhuan Depression was established (Figure 8).

In the Sh-1 member, the scale of the channel belt was relatively limited, with an average of 720~1,800 m (Table 2). The slope of the terrain was small, and the sand-carrying capacity was limited due to the weak hydrodynamic conditions. The warm and humid climate was suitable for vegetation growth (Zhu et al., 2020). The soil consolidation in the provenance area was quite stable, the sediment supply was

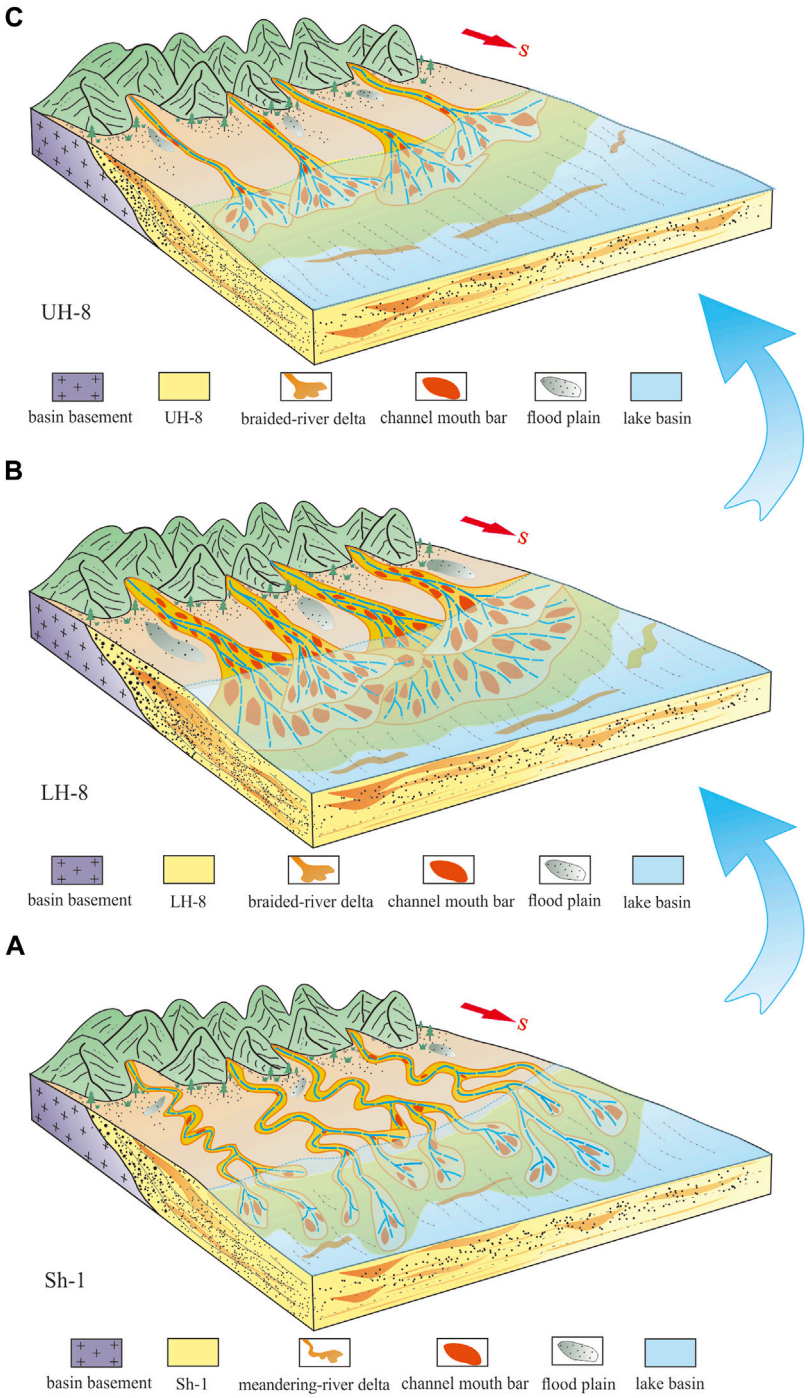

FIGURE 8
Sedimentary evolution model of the delta in the Sh-1 to He-8 members in the Tianhuan Depression, the Ordos Basin. **(A)** Sedimentary environment of the Sh-1 member, **(B)** sedimentary environment of the LH-8 member, and **(C)** sedimentary environment of the UH-8 member.

weakened, leading to a decline in the lateral migration ability of rivers, and the meandering river delta sediments were limited in size and were mostly isolated sand bodies (Figure 8A).

In the LH-8 member, the river sedimentation was suddenly enhanced due to the strong drop in the lake base level; the sediment supply was adequate, and the deposition rate was rapid. The strong hydrodynamic conditions and rapid sediment supply

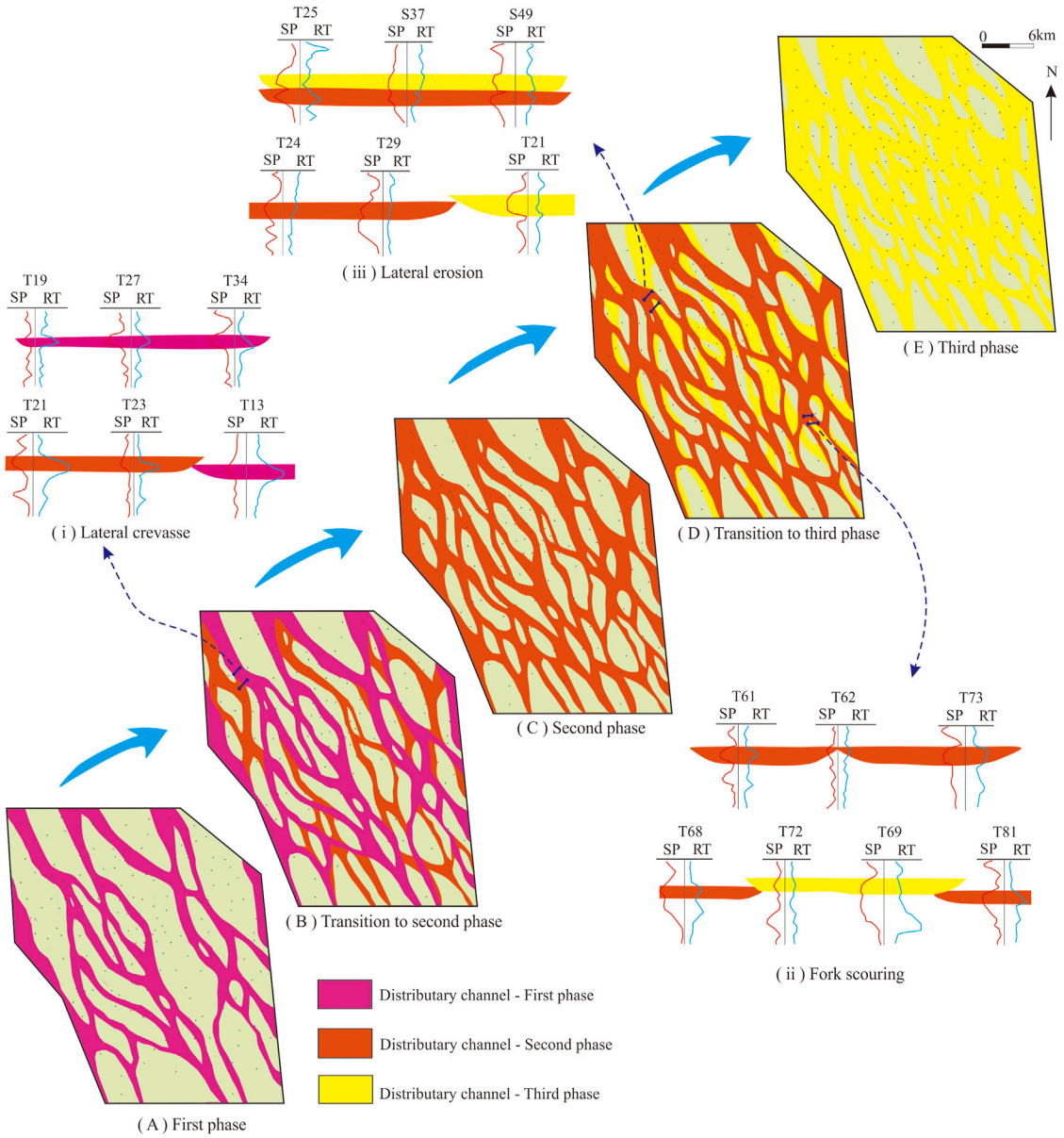

FIGURE 9
Evolution of distributary channels and single sand body architecture and genesis mechanisms in the LH-8 member. (i, ii, iii) are the three single sand body architecture models, **(A,C,E)** are the three phase distributary channels, and **(B,D)** are the transitional phases.

led to a lack of time for the "digestion" of main transport channels, thus forming large braided river deltas. More importantly, with the further increase of the paleo-slope (Zhang et al., 2018), the hydrodynamic conditions strengthened again, leading to the forward transport or lateral migration of the underwater distributary channels. The channel frequently bifurcated and then intersected, and the underwater parts were prone to forming superimposed sand bodies (mainly vertically superimposed and laterally tangentially superimposed; Figure 8B).

In the UH-8 member, the lake datum was at a high level during the deposition period when compared with that of the LH-8 member. As the slope became gentler (Zhang et al., 2018), the hydrodynamic conditions weakened and the sediment supply decreased, leading to a decline in the lateral erosion capacity of the channel. At this time, the sedimentary environment was still a braided river delta, but the channel scale was weaker than that of the LH-8 member, with the underwater parts mostly forming horizontally bridged sand bodies (Figure 8C).

5.2 Genetic analysis of the single sand body

The stacking styles of different single sand bodies are the products of distributary channel evolution (Marzo et al., 1988; Joeckel et al., 2016). The analysis of channel evolution patterns will help to clarify the sand bodies' configuration and genesis. According to the difference in channel elevation and sedimentary microfacies at different stages identified by logging, the channel evolution in the study area mainly had the following three models (Figure 9).

i) Lateral crevasse at the riverside

The lateral crevasse, formed during intermittent flood periods, was caused by the river bursting the concave banks when the water level of the original channel rose (Figure 9(i)). The scale of the crevasse channel was generally smaller than the original channel, and the angle between the mainstream direction and the original channel was smaller. The lateral crevasse could form a new channel and then evolve from the original isolated sand body to laterally tangentially superimposed sand bodies, which play a crucial role in the overall widening of the channel.

ii) Inter-channel fork scouring at the river front

Fork scouring was caused by continuous erosion of the original river fork area (Figure 9 (ii)). The main upstream channel was uninterruptedly scoured, reconstructed the bifurcation, which could erode the inter-river floodplain and develop new channels under appropriate conditions, and then evolved from original horizontally bridged sand bodies to laterally tangentially superimposed sand bodies, thus enlarging the channel scope, enhancing the flood discharge capacity, and reaching a new balance of the channel.

(iii) Lateral erosion at the riverside

Lateral erosion was a common channel evolution mode, which was caused by the lateral circulation of the original channel (Figure 9 (iii)). The lateral erosion occurred only in a certain section (the angle of flow direction is suddenly greater than 15°) of the original channel and may evolve into a new crevasse channel, so vertically superimposed and laterally tangentially superimposed sand bodies are often developed.

During the formation of the contemporaneous compound channels, the late channels developed on the basis of the early channels, and thus their top elevations were generally higher than those of the early rivers (Sahoo et al., 2016; Qin et al., 2017). The LH-8 member is one of the most interesting layers due to its diverse sand body stacking patterns and complex channel networks; hence, the evolution process of the distributary channel was specially established in the LH-8 member, which experienced three main stages of evolution (Figure 9).

The first phase is the initial developing stage of distributary channels (Figure 9A), and it can be seen that four main distributary channels developed from the provenance direction (NW direction). The northern distributary channels were larger in scale, with bifurcation-merger evident in the middle of the rivers, while the southern distributary channels were smaller in scale and mostly isolated. During the transitional stage (Figure 9B), the northern distributary channels widened significantly, and crevasse erosion was dominant in the near-provenance area, resulting in the large-scale distribution of channels in the northwest. The original distributary channels in the central part of the study area had varying degrees of crevasse erosion and lateral erosion, but the scale was small, and the sand bodies were mostly of the laterally tangentially superimposed type.

In the second phase (Figure 9C), the characteristics of distributary channels were still clearly visible. The distribution of the former southern distributary channels became larger, the southern channels were dominated by lateral erosion, and the scale of distributary channels further increased. At this time, the single distributary channel was dominated by the horizontally bridged type (Figure 9D).

In the third phase (Figure 9E), the new channels were mainly formed by lateral erosion on the basis of the second-stage channels. According to the distribution of channels during the transition period, there were notable large-scale crevasses between the original distributary channels only near the provenance, and most of them were lateral crevasses in the middle of the study area. The phenomenon of inter-channel fork erosion also appeared during this period. During the third stage, the distributary channel features were not evident, and the channels as a whole were interleaved into a sheet spread. The width and size of the channels reach their maximum, and the vertical superposition of distributary channels in different periods could be seen, which also explained that the sand bodies were mostly vertically superimposed in the current LH-8 member.

5.3 Geological implications for natural gas exploitation

Different single sand body architectures represent different natural gas accumulation conditions, which will also cause differences in gas/water enrichment in sand bodies. The gas reservoir profile of wells T34–S38 shows that the sand bodies in the LH-8 member are superior to those of the UH-8 and Sh-1 members in terms of size and vertical and horizontal connectivity (Figure 10). The LH-8 reservoir is mainly composed of gas and water layers or water-bearing gas layers, while the sand bodies of the UH-8 member are mostly dominated by gas and water layers and dry layers, and the sand bodies are mostly isolated or horizontally

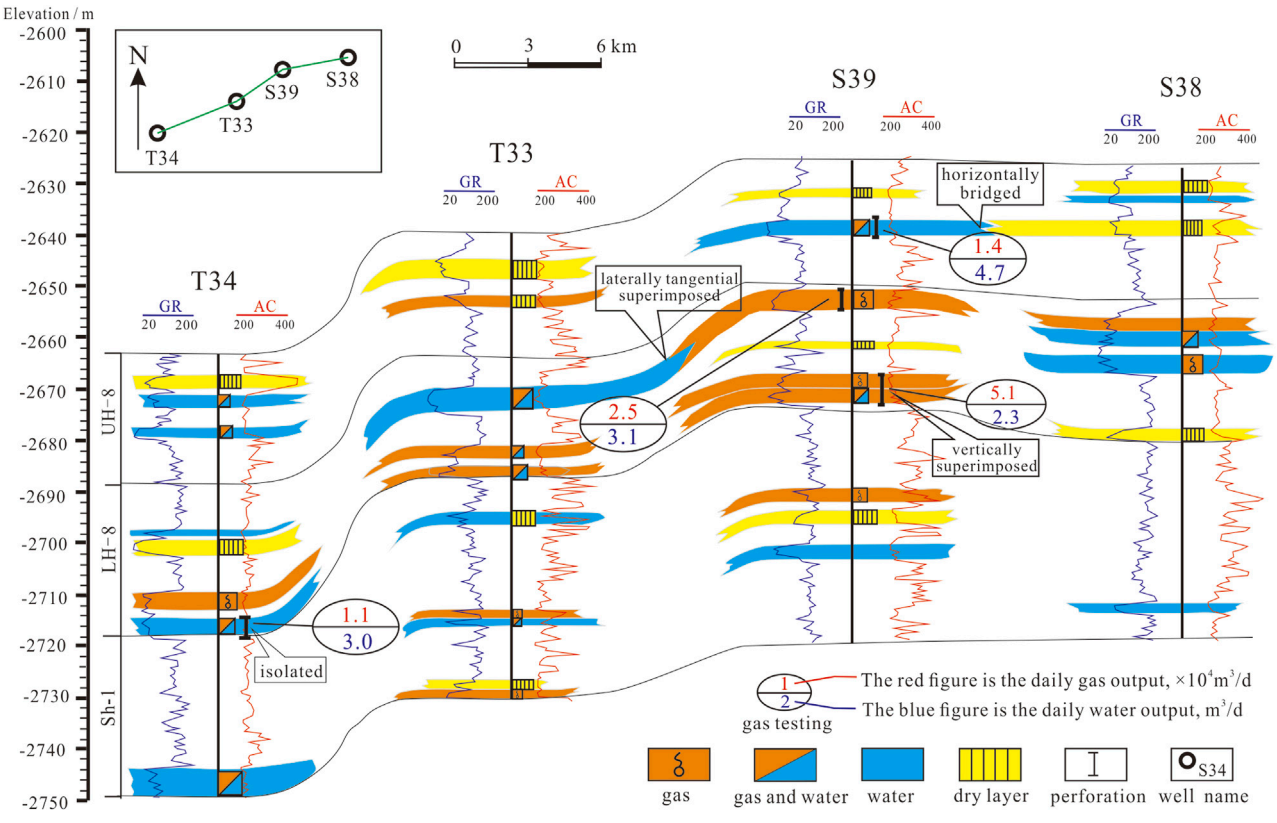

FIGURE 10
Gas reservoir profile of wells T34–S38 in the study area.

bridged, with relatively poor connectivity. The Sh-1 member is dominated by gas and water layers with isolated sand bodies and poor connectivity. The gas testing results show that when the topographic structure and source rock conditions are similar, the vertically superimposed sand bodies have the largest gas production, followed by the laterally tangentially superimposed sand bodies, and the isolated and horizontally bridged sand bodies have the least gas saturation.

According to the statistical results of well logging and gas testing, the vertically superimposed and laterally tangentially superimposed sand bodies are mostly enriched in natural gas (Figure 10), which is due to the vertically superimposed sand bodies that have been washed and superimposed by multi-stage distributary channels, forming good lithology–physical properties vertically. In addition, if the gas supply from the underlying hydrocarbon rocks is sufficient or the transport channel is open, it is conducive to the enrichment of natural gas. The tangentially superimposed sand bodies not only have superior connectivity laterally but can also form a relatively good lithology–physical property combination vertically, which is also conducive to the accumulation of natural gas. However, the isolated and horizontally bridged sand bodies are mostly surrounded by impermeable layers, making it difficult for gas to be filled, so the original sedimentary water is mostly retained. Therefore, combined with the current status of exploration and development, the next step in the study area will be to focus on the central parts of the distributary channels, especially the superimposed sand bodies. This work is instructive for basins with the same sedimentary and sand body genesis worldwide and thus has potentially significant scientific and development implications.

6 Conclusion

Single sand body architectures are crucial for the exploitation of tight sandstone gas (TSG) reservoirs. The stacking relationship of sand bodies from Sh-1 to He-8 members in the NT is divided into four main types: isolated, vertically superimposed, laterally tangentially superimposed, and horizontally bridged sand bodies.

Delta plain and front sub-facies are mainly deposited in the study area, and three kinds of sedimentary

microfacies are mainly developed: the distributary channel, the channel mouth bar, and the interdistributary bay. There are great differences in the development frequency of single sand body stacking patterns in different sedimentary microfacies.

The sedimentary evolution model is a complete cycle of river evolution from small scale to large scale to terminal weakening. During the sedimentary period of the Sh-1 member, the sediment supply was insufficient, with restricted meandering river deltas dominating and sand bodies mostly existing as isolated types. Until the depositional period of the LH-8 member, the sediment supply increased suddenly, the deposition rate accelerated, and braided river delta deposition developed, generally forming superimposed sand bodies. By the depositional period of the UH-8 member, the provenance had decreased again. Although the sedimentary environment of the braided river delta had not changed substantially, the sand body distribution and channel scale were limited.

The stacking styles of different single sand bodies are the products of distributary channel evolution. The river evolution in the study area has the following three models: lateral crevasse at the river side, inter-channel fork scouring at the river front, and lateral erosion at the riverside, which plays a crucial role in the overall widening of the channel. Considering the current exploration and development status, the next step is to take the central parts of the distributary channels, especially the superimposed sand bodies, as the primary development target.

Data availability statement

The original contributions presented in the study are included in the article/Supplementary Material; further inquiries can be directed to the corresponding author.

Author contributions

ZY: writing—original draft, conceptualization, methods, and investigation. SW: data processing and editing. JC: formula calculation and review. SJ: outcrop data processing and well log interpretation.

Acknowledgments

We thank PetroChina Changqing Oilfield Company for permission to use well logging data and production data for this research. We also thank the Chief Editor Valerio Acocella, the Associate Editor Lawrence H. Tanner, and two reviewers for their valuable comments and constructive modifications that greatly enhanced the manuscript.

Conflict of interest

SW was employed by the company PetroChina Changqing Oilfield Company. SJ was employed by the company Shaanxi Yanchang Oil and Gas Exploration Company.

The remaining authors declare that the research was conducted in the absence of any commercial or financial relationships that could be construed as a potential conflict of interest.

Publisher's note

References

Aalto, R., Maurice-Bourgoin, L., Dunne, T., Montgomery, D. R., and Guyot, J. L. (2003). Episodic sediment accumulation on Amazonian flood plains influenced by El Nino/Southern Oscillation. *Nature* 425 (6957), 493–497. doi:10.1038/nature02002

Abdel, Z. A. (2021). Fluvial architecture of the Upper cretaceous Nubia Sandstones: An ancient example of sandy braided rivers in central Eastern Desert, Egypt. *Sediment. Geol.* 420, 105923–23. doi:10.1016/j.sedgeo.2021.105923

Allen, J. R. L. (1978). Studies in fluviatile sedimentation: An exploratory quantitative model for the architecture of avulsion-controlled alluvial suites. *Sediment. Geol.* 21, 129–147. doi:10.1016/0037-0738(78)90002-7

Aslan, A., Autin, W. J., and Blum, M. D. (2005). Causes of River Avulsion: Insights from the Late Holocene Avulsion History of the Mississippi River, U.S.A. *J. Sediment. Res.* 75 (4), 650–664. doi:10.2110/jsr.2005.053

Blum, M., Martin, J., Milliken, K., and Garvin, M. (2013). Paleovalley systems: Insights from Quaternary analogs and experiments. *Earth. Sci. Rev.* 116, 128–169. doi:10.1016/j.earscirev.2012.09.003

Colombera, L., and Mountney, N. P. (2021). Influence of fluvial crevasse-splay deposits on sandbody connectivity: Lessons from geological analogues and stochastic modelling. *Mar. Petroleum Geol.* 128, 105060–105123. doi:10.1016/j.marpetgeo.2021.105060

Coronel, M. D., Isla, M. F., Veiga, G. D., Mountney, N. P., Colombera, L., and Ghinassi, M. (2020). Anatomy and facies distribution of terminal lobes in ephemeral fluvial successions: Jurassic Tordillo Formation, Neuquén Basin, Argentina. *Sedimentology* 67 (5), 2596–2624. doi:10.1111/sed.12712

Dai, J., Li, J., Wang, B., and Pan, R. (2012). Distribution regularity and formation mechanism of gas and water in the Western area of Sulige gas field, NW China. *Petroleum Explor. Dev.* 39 (5), 560–566. doi:10.1016/s1876-3804(12)60076-7

Dalrymple, R. W., and Choi, K. (2007). Morphologic and facies trends through the fluvial–marine transition in tide-dominated depositional systems: A schematic framework for environmental and sequence-stratigraphic interpretation. *Earth-Science Rev.* 81 (3-4), 135–174. doi:10.1016/j.earscirev.2006.10.002

El-Ghali, M., Morad, S., Mansurbeg, H., Caja, M. A., Ajdanlijsky, G., Ogle, N., et al. (2009). Distribution of diagenetic alterations within depositional facies and sequence stratigraphic framework of fluvial sandstones: Evidence from the

Petrohan Terrigenous Group, Lower Triassic, NW Bulgaria. *Mar. Petroleum Geol.* 26 (7), 1212–1227. doi:10.1016/j.marpetgeo.2008.08.003

Fernandes, A. M., Tornqvist, T. E., Straub, K. M., and Mohrig, D. (2016). Connecting the backwater hydraulics of coastal rivers to fluvio-deltaic sedimentology and stratigraphy. *Geology* 44, 979–982. doi:10.1130/g37965.1

Flood, Y. S., and Hampson, G. J. (2017). Analysis of floodplain sedimentation, avulsion style and channelized fluvial sandbody distribution in an upper coastal plain reservoir: Middle Jurassic Ness Formation, Brent Field, UK North Sea. *Geol. Soc. Lond. Spec. Publ.* 444 (1), 109–140. doi:10.1144/sp444.3

Flood, Y. S., and Hampson, G. J. (2015). Quantitative Analysis of the Dimensions and Distribution of Channelized Fluvial Sandbodies Within A Large Outcrop Dataset: Upper Cretaceous Blackhawk Formation, Wasatch Plateau, Central Utah, U.S.A. *J. Sediment. Res.* 85 (4), 315–336. doi:10.2110/jsr.2015.25

Galina, M., and Norman, S. (2000). Holocene avulsion styles and sedimentation patterns of the Saskatchewan River, Cumberland Marshes, Canada. *Sediment. Geol.* 130 (1-2), 81–105. doi:10.1016/s0037-0738(99)00106-2

Gao, Y., Wang, Z., Yi, S., She, Y., Lin, S., Li, M., et al. (2019). Mineral characteristic of rocks and its impact on the reservoir quality of He 8 tight sandstone of Tianhuan area. *Ordos Basin Nat. Gas. Geosci.* 30 (3), 344–352.

Gibling, M. R. (2006). Width and Thickness of Fluvial Channel Bodies and Valley Fills in the Geological Record: A Literature Compilation and Classification. *J. Sediment. Res.* 76 (5), 731–770. doi:10.2110/jsr.2006.060

Guo, Y., Pang, X., Li, Z., Guo, F., and Song, L. (2016). The critical buoyancy threshold for tight sandstone gas entrapment: physical simulation, interpretation, and implications to the Upper Paleozoic Ordos Basin. *J. Petroleum Sci. Eng.* 149, 88–97. doi:10.1016/j.petrol.2016.10.004

Hajek, E. A., and Edmonds, D. A. (2014). Is river avulsion style controlled by floodplain morphodynamics? *Geology* 42 (3), 199–202. doi:10.1130/g35045.1

Hajek, E. A., and Wolinsky, M. A. (2012). Simplified process modeling of river avulsion and alluvial architecture: Connecting models and field data. *Sediment. Geol.* 257-260, 1–30. doi:10.1016/j.sedgeo.2011.09.005

Hampson, G. J., Royhan Gani, M., Sahoo, H., Rittersbacher, A., Irfan, N., Ranson, A., et al. (2012). Controls on large-scale patterns of fluvial sandbody distribution in alluvial to coastal plain strata: Upper Cretaceous Blackhawk Formation, Wasatch Plateau, Central Utah, USA. *Sedimentology* 59, 2226–2258. doi:10.1111/j.1365-3091.2012.01342.x

Heidsiek, M., Butscher, C., Blum, P., and Fischer, C. (2020). Small-scale diagenetic facies heterogeneity controls porosity and permeability pattern in reservoir sandstones. *Environ. Earth Sci.* 79 (18), 425–427. doi:10.1007/s12665-020-09168-z

Hovadik, J. M., and Larue, D. K. (2007). Static characterizations of reservoirs: refining the concepts of connectivity and continuity. *Pet. Geosci.* 13 (3), 195–211. doi:10.1144/1354-079305-697

Jerolmack, D. J., and Mohrig, D. (2007). Conditions for branching in depositional rivers. *Geol.* 35, 463–466. doi:10.1130/g23308a.1

Joeckel, R. M., Tucker, S. T., and McMullin, J. D. (2016). Morphosedimentary features from a major flood on a small, lower-sinuosity, single-thread river: The unknown quantity of overbank deposition, historical-change context, and comparisons with a multichannel river. *Sediment. Geol.* 343 (15), 18–37. doi:10.1016/j.sedgeo.2016.07.010

Khalifa, M. K., and Mills, K. J. (2020). Facies analysis relationships depositional environments of the subsurface stratigraphy of the Snake Cave Interval in the Bancannia Trough, Western Darling Basin, New South Wales, SE Australia. *Mar. Petroleum Geol.* 115, 104279–104324. doi:10.1016/j.marpetgeo.2020.104279

Marion, P., Yan, N., Luca, C., Nigel, P. M., Pauline, C., and Guillaume, C. (2020). Combined inverse and forward numerical modelling for reconstruction of channel evolution and facies distributions in fluvial meander-belt deposits. *Mar. Petroleum Geol.* 117, 104409–104415. doi:10.1016/j.marpetgeo.2020.104409

Marzo, M., Nijman, W., and Puigdefabregas, C. (1988). Architecture of the Castissent fluvial sheet sandstones, Eocene, South Pyrenees, Spain. *Sedimentology* 35, 719–738. doi:10.1111/j.1365-3091.1988.tb01247.x

Meng, D., Jia, A., Ji, G., and He, D. (2016). Water and gas distribution and its controlling factors of large scale tight sand gas fields: A case study of Western Sulige gas field, Ordos Basin, NW China. *Petroleum Explor. Dev.* 43 (4), 663–671. doi:10.1016/s1876-3804(16)30077-5

Miall, A. D. (1977). A review of the Braided River Depositional Environment. *Earth. Sci. Rev.* 13 (1), 1–62. doi:10.1016/0012-8252(77)90055-1

Pisel, J. R., Pyles, D. R., Kirschbaum, M. A., and Marzo, M. (2018). The influence of lateral topographic confinement on fluvial channel-belt clustering, compensation and connectivity - lower Wasatch Formation and Dakota Sandstone, Utah, USA. *Sedimentology* 65, 597–619. doi:10.1111/sed.12395

Pranter, M. J., Cole, R. D., Panjaitan, H., and Sommer, N. K. (2009). Sandstone-body dimensions in a lower coastal-plain depositional setting: Lower Williams Fork Formation, Coal Canyon, Piceance Basin, Colorado. *Am. Assoc. Pet. Geol. Bull.* 93, 1379–1401. doi:10.1306/06240908173

Pranter, M. J., and Sommer, N. K. (2011). Static connectivity of fluvial sandstones in a lower coastal-plain setting: An example from the Upper Cretaceous lower Williams Fork Formation, Piceance Basin, Colorado. *Am. Assoc. Pet. Geol. Bull.* 95 (6), 899–923. doi:10.1306/12091010008

Qin, G., Wu, S., Song, X., Zou, C., Zheng, L., and Chen, C. (2017). Sedimentary characteristics of distal fine-grain braided delta and architecture analysis of single sand body. *J. China Univ. Petroleum (Ed. Nat. Sci.* 41 (6), 9–19. doi:10.3969/j.issn.1673-5005.2017.06.002

Roberts, E. M. (2007). Facies architecture and depositional environments of the Upper Cretaceous Kaiparowits Formation, southern Utah. *Sediment. Geol.* 197 (3-4), 207–233. doi:10.1016/j.sedgeo.2006.10.001

Sahoo, H., Gani, M. R., Gani, N. D., Hampson, G. J., Howell, J. A., Storms, J. E. A., et al. (2020). Predictable patterns in stacking and distribution of channelized fluvial sand bodies linked to channel mobility and avulsion processes. *Geology* 48 (9), 903–907. doi:10.1130/g47236.1

Sahoo, H., Gani, M. R., Hampson, G. J., Gani, N. D., and Ranson, A. (2016). Facies- to sandbody-scale heterogeneity in a tight-gas fluvial reservoir analog: Blackhawk Formation, Wasatch Plateau, Utah, USA. *Mar. Petroleum Geol.* 78, 48–69. doi:10.1016/j.marpetgeo.2016.02.005

Shen, Z., Trnqvist, T. E., Mauz, B., Chamberlain, E. L., and Sandoval, L. (2015). Episodic overbank deposition as a dominant mechanism of floodplain and delta-plain aggradation. *Geology* 43 (10), 875–878. doi:10.1130/g36847.1

Slingerland, R., and Smith, N. D. (1998). Necessary conditions for a meandering-river avulsion. *Geol.* 26, 435–438. doi:10.1130/0091-7613(1998)026<0435:ncfamr>2.3.co;2

Snedden, J. W. (2013). Channel-body basal scours: Observations from 3D seismic and importance for subsurface reservoir connectivity. *Mar. Petroleum Geol.* 39 (1), 150–163. doi:10.1016/j.marpetgeo.2012.08.013

Syvitski, J. P., Overeem, I., Brakenridge, G. R., and Hannon, M. (2012). Floods, floodplains, delta plains — A satellite imaging approach. *Sediment. Geol.* 267-268 (1), 1–14. doi:10.1016/j.sedgeo.2012.05.014

Tian, J., Wu, Q., Wang, F., Lin, X., Zhang, J., and Cao, T. (2011). Research on development factors and the deposition Model of large area reservoir sandstones of He8 section of Xiashihezi Formation of Permian in Ordos basin. *Acta Petrol. Sin.* 27 (8), 2403–2412. doi:10.1134/S1075701511030068

Tian, J., Zhang, X., Wang, F., Chen, R., and Lin, X. (2013). Quantitative characterization of superimposition relationship and distribution of reservoir sandbodies in the Upper Palaeozoic of Gaoqiao region. *Ordos Basin Oil Gas Geol.* 34 (6), 737–842. doi:10.11743/ogg20130604

Toorenenburg, K. V., Donselaar, M. E., Noordijk, N. A., and Weltje, G. J. (2016). On the origin of crevasse-splay amalgamation in the Huesca fluvial fan (Ebro Basin, Spain): Implications for connectivity in low net-to-gross fluvial deposits. *Sediment. Geol.* 343 (15), 156–164. doi:10.1016/j.sedgeo.2016.08.008

Trendell, A. M., Atchley, S. C., and Nordt, L. C. (2013). Facies Analysis of A Probable Large-Fluvial-Fan Depositional System: The Upper Triassic Chinle Formation At Petrified Forest National Park, Arizona, U.S.A. *J. Sediment. Res.* 83 (10), 873–895. doi:10.2110/jsr.2013.55

Turner, B. R., and Tester, G. N. (2006). The Table Rocks Sandstone: A fluvial, friction-dominated lobate mouth bar sandbody in the Westphalian B Coal Measures, NE England. *Sediment. Geol.* 190 (1), 97–119. doi:10.1016/j.sedgeo.2006.05.007

Tye, R. S. (2013). Quantitatively Modeling Alluvial Strata for Reservoir Development with Examples from Krasnoleninskoye Field, Russia. *J. Coast. Res.* 69, 129–152. doi:10.2112/si_69_10

Weerts, H. J. T., and Bierkens, M. F. P. (1993). Geostatistical analysis of overbank deposits of anastomosing and meandering fluvial systems; Rhine-Meuse delta, The Netherlands. *Sediment. Geol.* 85 (1-4), 221–232. doi:10.1016/0037-0738(93)90085-j

Widera, M. (2016). Depositional environments of overbank sedimentation in the lignite-bearing Grey Clays Member: New evidence from Middle Miocene deposits of central Poland. *Sediment. Geol.* 335, 150–165. doi:10.1016/j.sedgeo.2016.02.013

Xiao, X. M., Zhao, B. Q., Thu, Z. L., Song, Z. G., and Wilkins, R. W. T. (2005). Upper Paleozoic petroleum system, Ordos Basin, China. *Mar. Petroleum Geol.* 22 (8), 945–963. doi:10.1016/j.marpetgeo.2005.04.001

Yang, H., Fu, J., Liu, X., and Meng, P. (2012). Accumulation conditions and exploration and development of tight gas in the Upper Paleozoic of the Ordos Basin. *Petroleum Explor. Dev.* 39 (3), 315–324. doi:10.1016/s1876-3804(12)60047-0

Yang, H., Fu, J., Wei, X., and Liu, X. (2008). Sulige field in the Ordos Basin : Geological setting, field discovery and tight gas reservoirs. *Mar. Petroleum Geol.* 25 (4-5), 387–400. doi:10.1016/j.marpetgeo.2008.01.007

Zhang, F., Li, J., Wei, G., Liu, X., Guo, J., Li, J., et al. (2018). Formation mechanism of tight sandstone gas in areas of low hydrocarbon generation intensity: A case study of the Upper Paleozoic in north Tianhuan depression in Ordos Basin, NW China. *Petroleum Explor. Dev.* 45 (1), 79–87. doi:10.1016/s1876-3804(18)30007-7

Zhou, Y., Ji, Y., Xu, L., Che, S., Niu, X., Wan, L., et al. (2016). Controls on reservoir heterogeneity of tight sand oil reservoirs in Upper Triassic Yanchang Formation in Longdong Area, southwest Ordos Basin, China: Implications for reservoir quality prediction and oil accumulation. *Mar. Petroleum Geol.* 78, 110–135. doi:10.1016/j.marpetgeo.2016.09.006

Zhu, S., Zhu, X., Jia, Y., Cui, H., and Wang, W. (2020). Diagenetic alteration, pore-throat network, and reservoir quality of tight gas sandstone reservoirs: A case study of the upper Paleozoic sequence in the northern Tianhuan depression in the Ordos Basin, China. *Am. Assoc. Pet. Geol. Bull.* 104 (11), 2297–2324. doi:10.1306/08151919058

Zhu, X., Deng, X., Liu, Z., Sun, B., Liao, J., and Hui, X. (2013). Sedimentary characteristics and model of shallow braided delta in large-scale lacustrine: An example from Triassic Yanchang Formation in Ordos Basin. *Earth Sci. Front.* 20 (2), 19–28. CNKI:SUN:DXQY.0.2013-02-005